Available online at www.sciencedirect.com

ScienceDirect

Procedia Engineering 204 (2017) 405–412

Procedia Engineering

www.elsevier.com/locate/procedia

14th Hypervelocity Impact Symposium 2017, HVIS2017, 24-28 April 2017, Canterbury, Kent, UK

Impact-induced compaction of primitive solar system solids: The need for mesoscale modelling and experiments

Thomas M. Davison[a,*], James G. Derrick[a], Gareth S. Collins[a], Philip A. Bland[b], Michael E. Rutherford[c], David J. Chapman[c], Daniel E. Eakins[c]

[a]*Impacts and Astromaterials Research Centre, Department of Earth Science and Engineering, Imperial College London, London, SW7 2AZ, UK*
[b]*Department of Applied Geology, Curtin University, GPO Box U1987, Perth, WA 6845, Australia*
[c]*Institute of Shock Physics, Imperial College London, SW7 2AZ UK*

Abstract

Primitive solar system solids were accreted as highly porous bimodal mixtures of mm-sized chondrules and sub-µm matrix grains. To understand the compaction and lithification of these materials by shock, it is necessary to investigate the process at the mesoscale; i.e., the scale of individual chondrules. Here we document simulations of hypervelocity compaction of primitive materials using the iSALE shock physics model. We compare the numerical methods employed here with shock compaction experiments involving bimodal mixtures of glass beads and silica powder and find good agreement in bulk material response between the experiments and models. The heterogeneous response to shock of bimodal porous mixtures with a composition more appropriate for primitive solids was subsequently investigated: strong temperature dichotomies between the chondrules and matrix were observed (non-porous chondrules remained largely cold, while the porous matrix saw temperature increases of 100's K). Matrix compaction was heterogeneous, and post-shock porosity was found to be lower on the lee-side of chondrules. The strain in the matrix was shown to be higher near the chondrule rims, in agreement with observations from meteorites. Chondrule flattening in the direction of the shock increases with increasing impact velocity, with flattened chondrules oriented with their semi-minor axis parallel to the shock direction.

Peer-review under responsibility of the scientific committee of the 14th Hypervelocity Impact Symposium 2017.

Keywords: Numerical methods; Mesoscale modeling; Shock compaction; Planetary science; Chondrites; Parent body processes

* Corresponding author. Tel.: +44 20 7594 2019; fax: +44 20 7594 7444.
E-mail address: thomas.davison@imperial.ac.uk

1877-7058
Peer-review under responsibility of the scientific committee of the 14th Hypervelocity Impact Symposium 2017.
10.1016/j.proeng.2017.09.801

Nomenclature

α	Distension
ε	Strain
ε_{xx}	Normal strain in *x*-direction
ε_{yy}	Normal strain in *y*-direction
ε_{xy}	Shear strain
P	Pressure
T	Temperature
v_i	Impact velocity
Y	Material cohesive strength
U_s	Shock velocity
u_p	Particle velocity

1. Introduction

Chondritic asteroids and meteorites are among the most primitive solar system objects, and provide our clearest record of solar system formation. While present-day asteroids are lithified, they would have accreted as highly porous [1,2] accumulates of two principal components: zero-porosity mm-sized spherical inclusions (chondrules) set within a high-porosity matrix of sub-μm dust grains. Meteorite shock classification schemes are a measure of how strongly the material has been shocked, but are calibrated against shock recovery experiments performed on geologic materials with little-to-no porosity [3]. Porous materials respond very differently to shock than non-porous materials [e.g. 4]. Furthermore, studies of meteorite shock level tend to determine shock metamorphic textures in the chondrules, with the assumption that if they are unshocked, so must be the matrix.

Carbonaceous chondrites are predominantly (85% of samples) classified as “unshocked” (< 4–5GPa) or “very weakly shocked” (5–10 GPa) [3,5]. Unequilibrated ordinary chondrites exhibit slightly higher shock levels, with 50% classified as “weakly shocked” (10–20 GPa) [3]. The inference commonly drawn from this is that these materials avoided high-intensity collisions, record no evidence of local pressure-temperature (*PT*) excursions and underwent little post-shock thermal metamorphism. However, it was recently proposed that the bimodal and highly porous nature of chondritic precursor material may imply substantial compaction-driven *PT* excursions, even in low-intensity impacts [7].

Here we apply mesoscale shock physics modelling [e.g. 6] and shock compaction experiments [14] to analog primordial chondritic materials to investigate, and compare, their heterogeneous response to shock [7,8]. We confirm that our numerical methods reproduce the bulk response observed in experiments, providing evidence that the simulated shock compaction is realistic. We subsequently show that in low-intensity shock events, using materials that replicate primordial matter more accurately, deformation of chondrules and compaction of porous matrix on the scale of individual chondrules can provide indicators of shock direction and magnitude. These results have significant implications for interpreting the chondritic meteorite record.

2. Methods

To investigate the dynamic compaction of primitive chondritic mixtures we performed a series of complementary laboratory and numerical experiments. A suite of analog experiments was performed, using a single-stage, light-gas gun, in which the compacted material was a mixture of silica powder and soda lime glass spheres. These materials are readily available and good mechanical analogs of chondritic material. A set of mesoscale numerical simulations was conducted to replicate and compare with these experiments. A further set of simulations extended the results of the experiments by using material models, and set up, more appropriate for the chemical composition of early solar system solids, and exploring higher shock pressure regimes.

2.1. Analog experiments

Shock compaction of analog materials was conducted at the European Synchrotron Radiation Facility (ESRF) using a light gas gun and was investigated *in-situ* using x-ray radiography [14]. The mixtures comprised of ~30 vol.% spherical Soda-Lime glass beads (analog to the chondrules), ~70 vol.% Sipernat silica powder (analog to the matrix; grain size ~7 μm, ~70% porosity; this varied between experiments) and had a bulk porosity of ~50%. Two average glass bead sizes were used in separate sets of experiments: 196 μm and 425 μm diameter. The experimental apparatus was cylindrically symmetric and consisted of a polycarbonate sabot (25 mm thick, 12.7 mm diameter) with a copper or polycarbonate flyer (2 mm x 12.7 mm) fixed to one end, which struck a polycarbonate driver (2 mm thick) at approximately 600 ms^{-1}. The driver carried a shockwave into the particle bed (4.4 mm x 9.8 mm diameter), which was held by an aluminium shell (1 mm thick) with a PMMA backer on the rear end (6 mm x 10 mm diameter). Bulk shock and particle velocities were measured directly from the radiographs, respectively, by comparing the shock front and driver/powder boundary positions in each radiograph to their initial positions and dividing by the elapsed time [14].

2.2. Mesoscale modelling

The iSALE shock physics code [9–11] was used to simulate mesoscale planar impact experiments [7,8], in which a shock wave was propagated through a chondrite-analog bimodal mixture of explicitly-resolved non-porous disks (the chondrules) surrounded by high-porosity matrix. Due to the large difference in length-scales between chondrules and pores in the matrix, matrix porosity was parameterised using the ε-α porous-compaction model [11,12]. Chondrules were placed with random sizes and spacing within the computational mesh until the desired matrix-to-chondrule volume ratio was reached.

Two sets of simulations were run. The first set accurately replicated the plate impact experiments described above and used the same experiment geometry, not including the aluminium container and PMMA window. The Mie-Grüneisen equation of state was used for all materials, including the solid component of the silica powder matrix. Material parameters for polycarbonate, soda lime glass and silica were used to represent the sabot/driver, chondrules, and matrix, respectively. Chondrule strength was treated as elastic-perfectly plastic, with a yield strength of 1 GPa. Bulk matrix strength was described using a Drucker-Prager strength model, with a friction coefficient of 0.7 and a cohesion of 0.01 MPa. Impact speeds ranging from v_i = 100—1300 ms^{-1} were used to generate a Hugoniot in $U_s - u_p$ space.

In the second set of simulations, to provide a closer analog for chondritic parent bodies, the ANEOS equation of state for forsterite [13] was used to describe the thermodynamic response of the chondrules and the solid component of the matrix. A strength model appropriate for geologic materials [10] was used in these simulations. Chondrules were assigned a high cohesive strength (1 GPa), and the porous matrix was very weak (cohesive strength of a few kPa; friction coefficient of 0.6). Impact velocity was varied over the interval v_i = 0.75–3 km/s; the initial matrix volume fraction was varied from 30–80% and the initial matrix porosity was typically set to 70%, although some simulations explored this parameter, ranging from 60–80%. The initial temperature was 300 K (changing the initial temperature had a minimal effect on the temperature changes experienced by the material).

The forsterite simulations used a different experiment geometry compared to the silica simulations/experiments, consistent with previous work [7,8]. In this case, the flyer plate (thickness 30 mm), driver plate (15 mm) and sample plate (15 mm) all comprised the same material mixture. Beneath the sample plate, a buffer plate of length 20 mm was included to allow the shock wave to pass through the bottom of the sample without reflecting or releasing. With this geometry, a shock duration of around 20 – 30 μs is required in chondrite analog materials to allow the porosity, pressure, and temperature in the shock wave to reach a steady state [8]. The long impactor was required to delay the arrival of the release wave generated from its back edge until at least this time.

To track material histories, and thus record the peak- and post-shock state of the chondrules and matrix materials, Lagrangian tracer particles were placed throughout the sample region of the computational mesh. Bulk material properties were calculated from these tracer particles.

2.3. Quantifying strain and chondrule deformation

For the forsterite simualtions, the displacement of the Langragian tracer particles was extracted from the model, and used to quantify the strain of the material [15]. This is preferable to using the strain calculated as a cell-centered quantity on the Eulerian grid: The Eulerian method has no knowledge of the material history as it moves through the mesh, while Lagrangian tracers retain this information.

To calculate the tracer displacement, first a quadrilateral of nearest-neighbour tracers was found from the initial timestep: for each tracer that ended up in a region of interest at the end of the calculation, its initial coordinates were found (i, j), and then index of the closest tracers to the right (i+1, j), above (i, j+1) and diagonally above and to the right (i+1, j+1) were found. Second, the positions of these four tracers were found at the final timestep, and the displacement in the horizontal and vertical directions was calculated as the difference between the initial and final timestep locations. Finally, the three components of the total accumulated strain (ε_{xx}, ε_{yy}, ε_{xy}) were calculated from the tracer locations and displacements using the method outlined in [15], from which an invariant measure of the strain was also calculated.

To further quantify the amount of material deformation in the simulations, ellipses were fit to each chondrule in the sample region after shock and release, using a direct least-squares fitting method, specific to ellipses [16], from which the chondrule eccentricity and orientation were derived.

3. Results

3.1. Comparison of iSALE mesoscale models with shock compaction experiments

The bulk response of the two suites of numerical simulations, using large and small chondrules, was extracted in U_s-u_p space (Fig 1). The two Hugoniot curves are in good agreement and do not differ significantly over the full range of particle velocities, which suggests that chondrule size does not affect the bulk response. This is reinforced by comparison of individual simulations, which show little difference in the positions of the shock front and driver/powder interface at equivalent times (Fig 2, Fig 3). Chondrule size does, however, affect heterogeneity at the shock front. Small-chondrule simulations display a ‘narrower’ shock front width (the difference between the maximum and minimum shock position across the bed at a given time; solid cyan line) compared to the equivalent large-chondrule simulations (Fig 2, Fig 3).

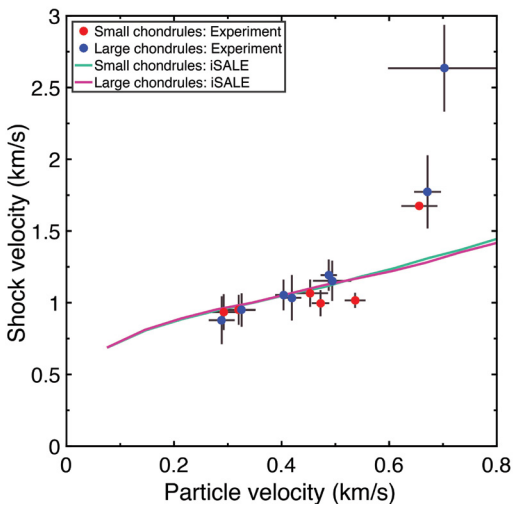

Fig 1: Numerically modelled Hugoniots extracted from iSALE compared with values from experiments [14] in U_s – u_p space for both large (~0.45 mm diameter) and small (~0.2 mm diameter) chondrules. Experimental error bars represent 95% of the distribution of velocity values that existed in the shocked mixtures.

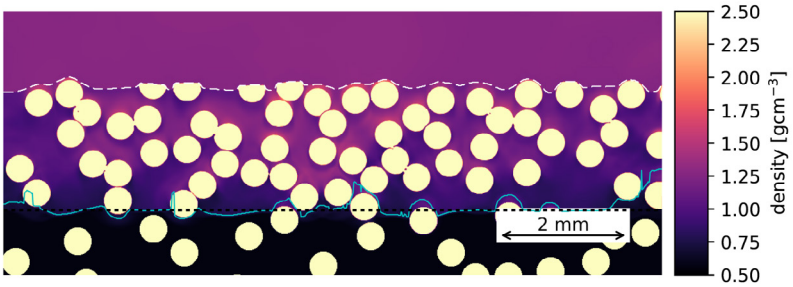

Fig 2: Density plot of the full, large chondrule, particle bed, based on experimental work [14], 3.45 μs after impact, for v_i = 600 ms^{-1} . The driver/powder interface is denoted by the dashed white line, the shock front across the bed by the solid cyan line, and the average shock front by the dashed black line; motion is down the image.

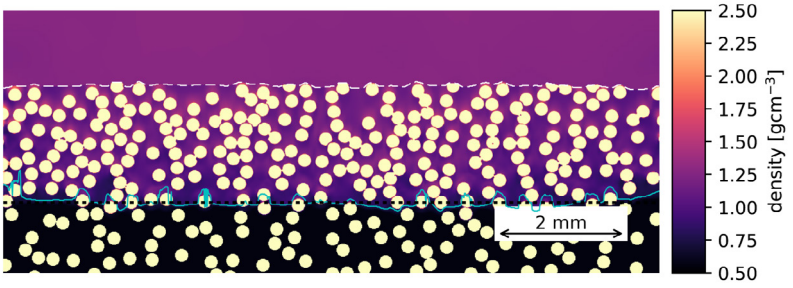

Fig 3: Density plot of the full, small chondrule, particle bed based on experimental work [14], 3.45 μs after impact, for v_i = 600 ms^{-1} . The driver/powder interface is denoted by the dashed white line, the shock front across the bed by the solid cyan line, and the average shock front by the dashed black line; motion is down the image.

The model and experimental results [14] compare favourably in U_s-u_p space (Fig 1). The model Hugoniot curves lie within experimental uncertainty but exhibit marginally higher shock speeds owing to the lack of lateral release in the simulations. Lateral release did not occur in the simulations because they did not resolve the full experimental geometry and only considered a central column of the experiment and used 'open' boundary conditions on the edges of the simulation. However, at high u_p there is a large difference between the model and experimental results. Analysis of the radiographs showed that this was because of non-uniform chondrule arrangements in some experiments, where the soda-lime spheres had 'bunched' at the impact surface of the sample [14]. The high density of soda-lime spheres produced a much faster shock through the mixture in that region. Overall, the good agreement of the modeled bulk response with the experimental data suggests that the mesoscale modeling approach is correctly capturing the compaction behavior in the analog chondritic mixtures.

3.2. Mesoscale response to shock of bimodal forsterite mixtures

The subsequent mesoscale simulations that used forsterite mixtures reveal mesoscale information about shock response that is not yet measurable in physical experiments. The results show how the pressure, temperature and porosity vary on the scale of individual chondrules (mm-scale) [7]. In all impact scenarios, there are large differences in the temperatures of the chondrules and matrix. For example, in a 2.0 km s^{-1} impact into a 70% forsterite matrix precursor with a matrix porosity of 70%, the chondrule peak pressure was ~ 7 GPa (a pressure not-easily detected in typical petrographic studies [3,5]). However, even at these low pressures, the matrix experienced a temperature increase (ΔT) of 800K (Fig 4a), while chondrules were virtually unheated (ΔT = 70 K). Significant pressure (up to 10 GPa) and temperature (> 1000 K) heterogeneities are observed over short length scales (10–100 μm). This is consistent with temperature maps produced from CR2 chondrite GRA 06100 using FIB-TEM analysis [7]. Final bulk properties (matrix abundance, porosity) are consistent with typical chondrites [8].

Compaction of matrix porosity is also heterogeneous: “shadow zones” on the lee side of chondrules exhibited less compaction of pore space than other regions of matrix (Fig 4b). The initial simulations appear to exhibit some faint evidence of this mesoscale feature as well (Fig 2, Fig 3). This suggests that further analysis of porosity distributions in chondrite matrices could be used as an indicator for shock direction.

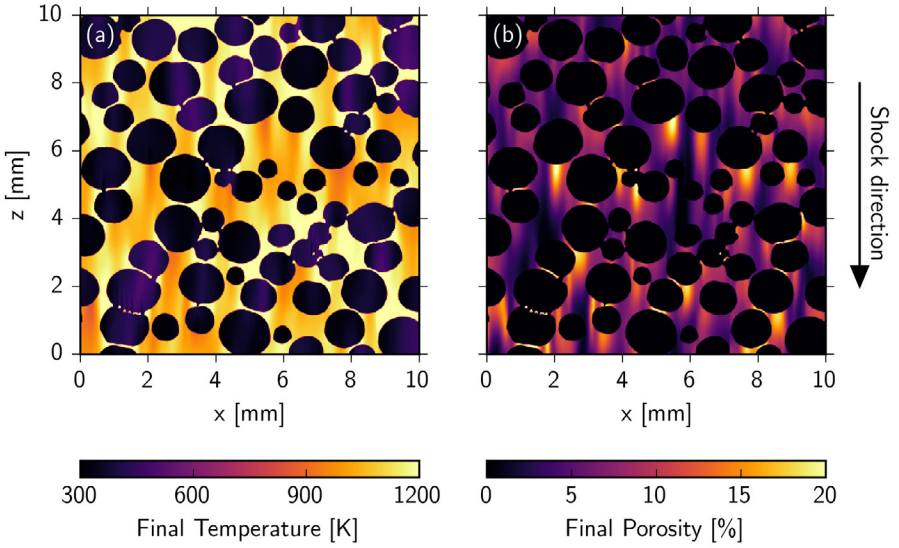

Fig 4: Final temperature (a) and porosity (b) distribution in a section of the sample material 30 μs after impact. Material started at 300K, and the matrix had an initial porosity of 70%.

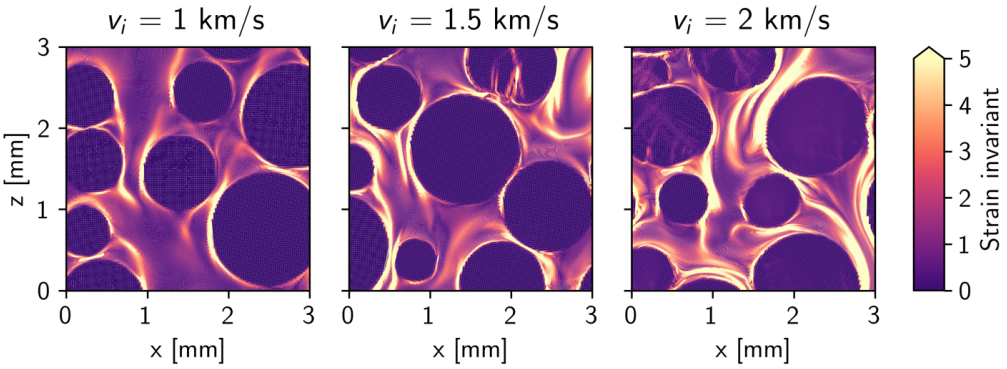

Fig 5: Accumulated total strain in simulations with three different velocities. Note that the matrix strain is highest near the chondrule rims. Deformation of the chondrules increases with increasing velocity, but is still small compared to the matrix

3.3. Strain

Using Lagrangian tracer particle positions, material strain was determined. The strain calculated here is a bulk strain, which in the matrix is a combination of the compaction of pore space and the strain in matrix grains. Strain in both the chondrules and the matrix increases with increasing impact velocity. The strain in the matrix is found to be much higher than in the chondrules, even at higher velocities (2 km s^{-1}) where the chondrules have been deformed

(Fig 5). Strain in the matrix is higher in the areas near chondrule rims. This was found to be in good qualitative agreement with strain calculated from Electron Backscatter Diffraction (EBSD) maps of the CV carbonaceous chondrite meteorite, Allende [17,18]. Eccentric and asymmetric strain shadows in the matrix may provide another shock-direction indicator.

3.4. Chondrule deformation

All chondrules in the sample region were fitted by ellipses [16]; for each ellipse, the eccentricity and orientation of the semi-major axis (relative to the shock propagation direction) were determined. Fig 6 shows the eccentricities and orientations of all ellipses calculated from simulations over a range of velocities (0.75, 1.0, 1.5, 2.0 and 2.5 km s^{-1}).

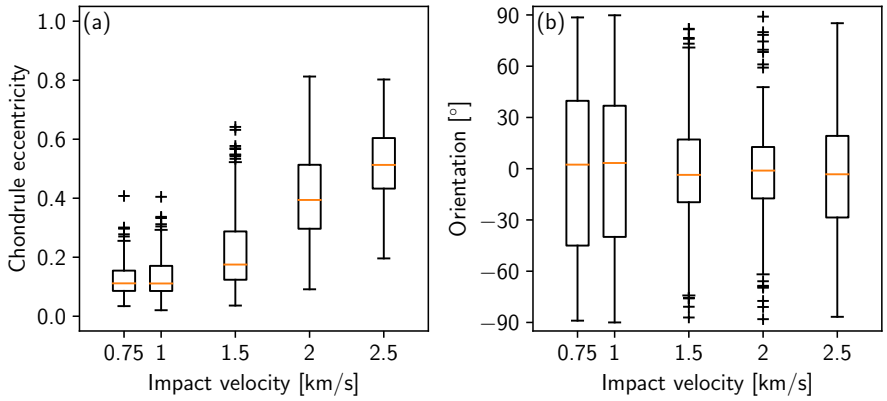

Fig 6: Box-and-whisker plots of (a) the eccentricity of post-shock chondrule shapes and (b) the ellipse orientation, as a function of velocity. Boxes extend from the lower to upper quartile. The orange line shows the median value. Whiskers extend to 1.5 times the inter-quartile range and black '+' symbols show data points outside that range. Ellipse orientation defines the angle between the ellipse semi-minor axis and the direction of shock propagation.

Chondrule eccentricity increases with increasing velocity. For $v_i \leq 1$ km s^{-1}, eccentricity is low (~0.1), and any elliptical chondrules are randomly oriented (since they are near-circular). At $v_i \geq 1.5$ km s^{-1}, the eccentricity increases (i.e. the chondrules have been flattened by the shock), and the range in orientation angles narrows; this shows that most chondrules have been preferentially flattened along an axis parallel to the shock propagation direction. Note that at $v_i = 2.5$ km s^{-1}, there is a small increase in the range of chondrule orientations; we attribute this to an increase in chondrule-chondrule collisions during shock compaction, leading to rotation of the chondrules after being flattened by the shock.

We note that the exact amount of chondrule deformation will depend on the assumed strength of the chondrules (in these simulations, Y_{chond} = 1GPa). Therefore, the transition from circular (spherical) to elliptical (oblate) chondrules will also vary with this strength; future shock compaction experiments could help to calibrate this for use as a shock magnitude indicator, and thus allow it to be used to derive an approximate shock pressure from chondrule-scale deformations.

4. Conclusions

Good agreement in bulk material response between mesoscale simulations and analog shock experiments provides evidence that our mesoscale approach correctly simulates the heterogeneous compaction of bimodal porous silica mixtures. Using more realistic analogs of primitive meteoritic material, our mesoscale compaction models are consistent with a range of meteoritic evidence, which suggests that chondritic meteorites, even those previously

labelled as unshocked or weakly shocked, may have undergone impact-induced compaction. The transient heating of matrix induced by low-intensity shock events would have led to lithification of primordial materials, and offers an alternative to compaction driven by hydrothermal alteration or lithostatic pressure.

Mesoscale modelling has revealed several potential shock-direction indicators:

- Compaction of porosity in the matrix on the lee-side of chondrules is lower than elsewhere in the surrounding matrix.
- Strain appears to be asymmetrically distributed around chondrules.
- Chondrules are flattened in the direction of shock propagation above a certain shock pressure (dependent on the chondrule strength). In the simulations presented here which assume a chondrule strength of 1 GPa, this occurs at an impact speed of ~1.5 km s^{-1}. Once flattened, chondrules tend to align their semi-minor axis along the direction of the shock wave propagation.

Further calibration of these indicators may provide an estimation of the direction and intensity of the shock to aid interpretation of meteoritic samples.

Acknowledgements

We thank the iSALE developers (www.isale-code.de) and the ESRF for their providing of the facilities necessary to perform the experimental work. TMD and GSC were supported by STFC grant ST/N000803/1. JGD is supported by EPSRC studentship funding. MER, DJC and DEE thank EPSRC and AWE for their support.

References

[1] P.A. Bland, L.E. Howard, D.J. Prior, J. Wheeler, R.M. Hough, K.A. Dyl, Earliest rock fabric formed in the Solar System preserved in a chondrule rim, Nature Geoscience. 4 (2011) 244–247.
[2] E. Beitz, C. Güttler, A.M. Nakamura, A. Tsuchiyama, J. Blum, Experiments on the consolidation of chondrites and the formation of dense rims around chondrules, Icarus. 225 (2013) 558–569.
[3] D. Stöffler, K. Keil, E.R.D. Scott, Shock metamorphism of ordinary chondrites, Geochimica et Cosmochimica Acta. 55 (1991) 3845–3867.
[4] T.G. Sharp, P.S. Decarli, Shock Effects in Meteorites, in: Meteorites and the Early Solar System II, University of Arizona Press, Tucson, 2006: pp. 653–677.
[5] E.R.D. Scott, K. Keil, D. Stöffler, Shock metamorphism of carbonaceous chondrites, Geochimica et Cosmochimica Acta. 56 (1992) 4281–4293.
[6] V.F. Nesterenko, Dynamics of Heterogeneous Materials, Springer, New York, 2001.
[7] P.A. Bland, G.S. Collins, T.M. Davison, N.M. Abreu, F.J. Ciesla, A.R. Muxworthy, J. Moore, Pressure–temperature evolution of primordial solar system solids during impact-induced compaction, Nat Commun. 5 (2014) 5451.
[8] T.M. Davison, G.S. Collins, P.A. Bland, Mesoscale numerical modeling of compaction of primitive solar system solids in low-velocity collisions, ApJ. 821 (2016) 68.
[9] A.A. Amsden, H.M. Ruppel, C.W. Hirt, SALE: A Simplified ALE computer program for fluid flow at all speeds, Los Alamos National Laboratories Report. LA-8095 (1980) 101p.
[10] G.S. Collins, H.J. Melosh, B.A. Ivanov, Modeling damage and deformation in impact simulations, Meteoritics & Planetary Science. 39 (2004) 217–231.
[11] K. Wünnemann, G.S. Collins, H.J. Melosh, A strain-based porosity model for use in hydrocode simulations of impacts and implications for transient crater growth in porous targets, Icarus. 180 (2006) 514–527.
[12] G.S. Collins, H.J. Melosh, K. Wünnemann, Improvements to the ε-α porous compaction model for simulating impacts into high-porosity solar system objects, International Journal of Impact Engineering. 38 (2011) 434–439.
[13] W. Benz, A.G.W. Cameron, H.J. Melosh, The origin of the Moon and the single-impact hypothesis III, Icarus. 81 (1989) 113–131.
[14] M.E. Rutherford, D.J. Chapman, J.G. Derrick, J.R.W. Patten, P.A. Bland, A. Rack, G.S. Collins, D.E. Eakins, Probing the early stages of shock-induced chondritic meteorite formation at the mesoscale, Scientific Reports. (In press).
[15] T.J. Bowling, PhD Thesis, Purdue University, 2015.
[16] A. Fitzgibbon, M. Pilu, R.B. Fisher, Direct least square fitting of ellipses, IEEE Transactions on Pattern Analysis and Machine Intelligence. 21 (1999) 476–480.
[17] L.V. Forman, P.A. Bland, N.E. Timms, G.S. Collins, T.M. Davison, F.J. Ciesla, G.K. Benedix, L. Daly, P.W. Trimby, L. Yang, S.P. Ringer, Hidden secrets of deformation: Impact-induced compaction within a CV chondrite, Earth and Planetary Science Letters. 452 (2016) 133–145.
[18] L.V. Forman, P.A. Bland, N.E. Timms, L. Daly, G.K. Benedix, P.W. Trimby, G.S. Collins, T.M. Davison, Defining the mechanism for compaction of the CV chondrite parent body, Geology. (In press).